



Project Report - Group 3

TECHNICAL-ECONOMIC FEASIBILITY STUDY OF A NEW HYDROPOWER PLANT TO BE INSTALLED AT THE
DOWNSTREAM END OF AN EXISTING WATER SUPPLY SYSTEM

HYDROPOWER SYSTEMS

Danilo Ramos (102167)
Davide Melozzi (102230)
Fabio Bentivogli (102376)

May 1, 2022

Contents

1	Technical Analysis: Hydraulic Calculations	2
2	Technical Analysis: Evaluation of Recovered Energy	4
3	Economic Analysis	7
4	Hydraulic Transient Analysis	9

1 Technical Analysis: Hydraulic Calculations

It is intended to build a hydroelectric plant at the downstream end of a water supply system, upstream of the arrival reservoir. The difference in elevations is about 136 m. A study was carried out to evaluate which technological solution for energy recovery is best suited to this situation. Thus, for a correct analysis, it is necessary to analyze the adducted flow records corresponding to a period of not less than 3 years (Figure 1), in order to adopt reliable models.

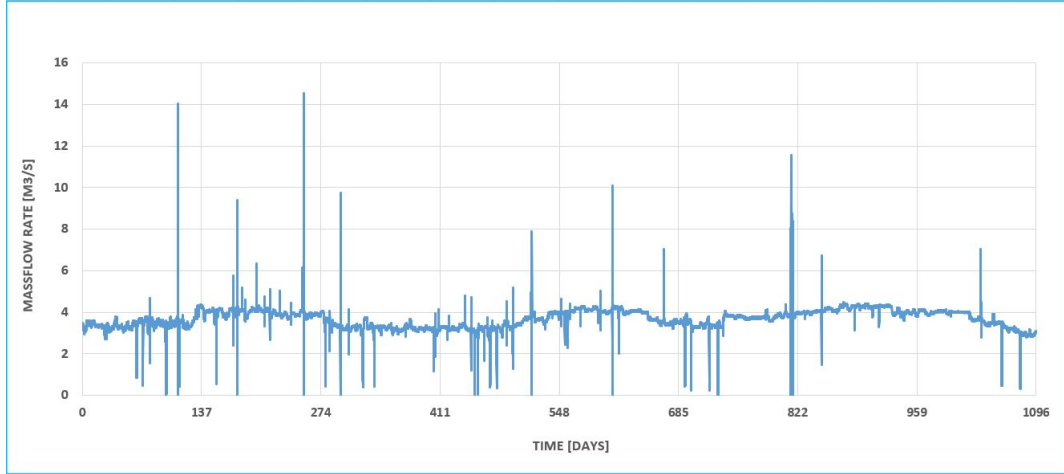


Figure 1: Flow variation as a function of time, triennium 2017-2019.

In Figure 1, it is possible to observe the existence of some atypical massflow rate values comparing to the others, which rise to values of approximately $15 \text{ m}^3/\text{s}$. These anomalous values correspond to operation maneuvers of the adductor or to errors in the reading of the flowmeter. The same figure shows the existence of warmer years in the triennium under analysis, as is the case of 2019, since that there is a correlation between water consumption and the thermal amplitudes that occurred in the respective year, while the years 2017 and 2018 correspond to cooler years for the reasons mentioned above.

For subsequent calculations, only the flow values inserted in the 5% and 95% percentile range will be considered, since they correspond to the values whose occurrence is greater, as shown in figure 2:

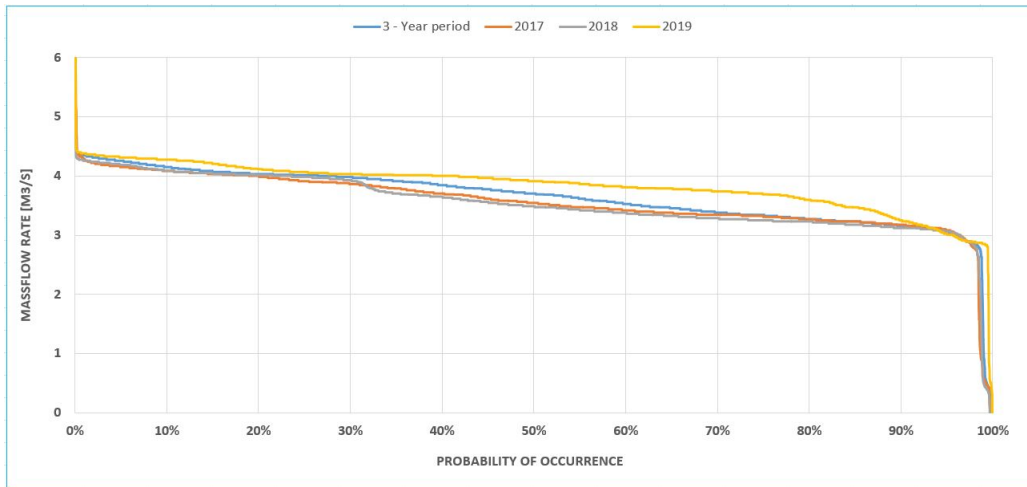


Figure 2: Probability of occurrence curve as a function of mass flow rate, triennium 2017-2019.

Then, the energy lines were drawn for the abovementioned flow range, in order to assess the existence of potential critical points along the pipe that could generate the phenomenon of cavitation and, thus, make the installation of the system technically unfeasible, since that it is a undesirable phenomenon due to the damages it may cause to its components where it occurs by erosion either on the blades of a turbine, pump or piston, originated by a pressure drop making the working fluid to reach its vaporization pressure.

By knowing the water level of the upstream reservoir ($Z_{\text{reservoir}} + 3 \text{ m}$) we have calculated the head losses by subtracting it from each part of the pipe. We highlight here the fact that the head losses were calculated by using Darcy-Weisbach formula:

$$h_L = f * \frac{L}{D} * \frac{V^2}{2g} \quad (1)$$

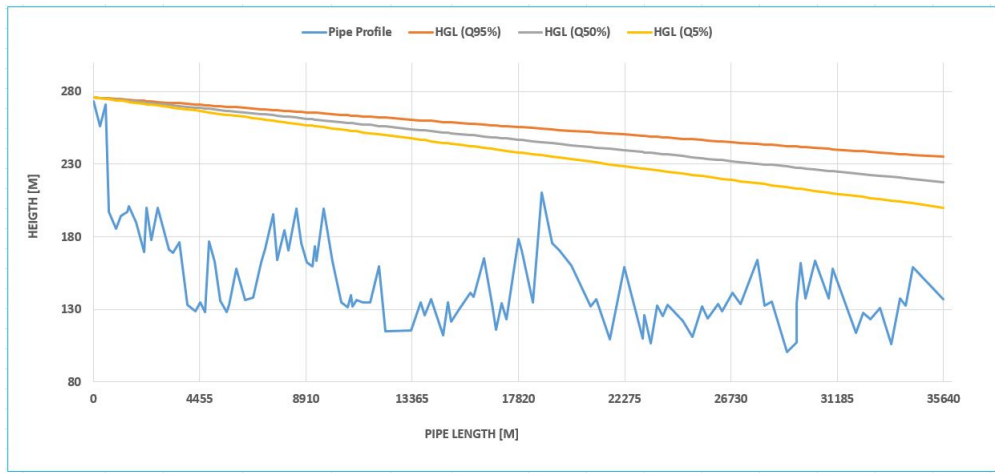


Figure 3: Energy lines for different mass flow ranges.

Since the nature of the study in question (economic feasibility), some simplifications were adopted to facilitate the analysis, without neglecting the minimum standards of rigor. It is noteworthy that, for this specific case, the Hydraulic grade line coincide with the respective Energy grade line due to the following assumption:

$$\frac{V^2}{2g} \approx 0 \quad (2)$$

Then, the possibility of installing a flow control safety valve was analyzed by calculating the head losses that it would introduce in the system, as well as the available power in the system to be turbined and the consequent produced energy for an uninterrupted period of 365 days a year, as shown in figure 4:

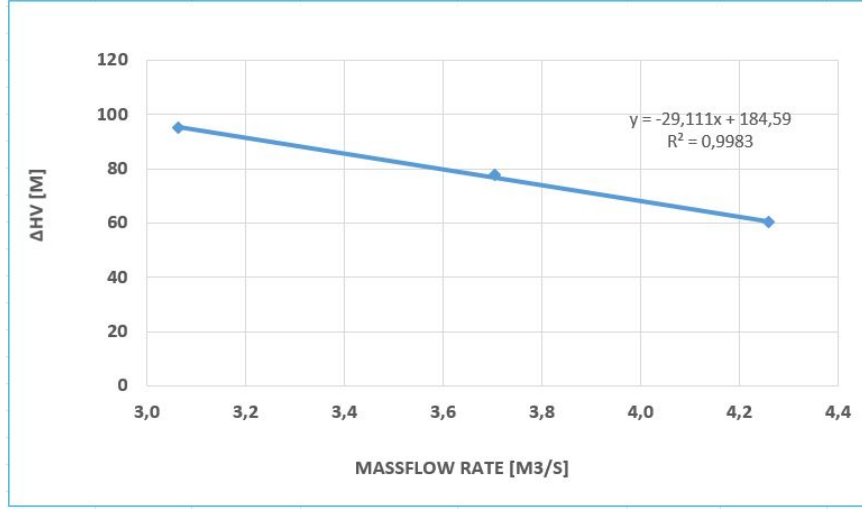


Figure 4: Energy lines for different mass flow ranges.

As expected, for higher mass flow rates, the greater the pressure drop in the valve, resulting in a “parabolic” type of downward trend.

Table 1: Turbined Power in function of mass flow rate

Percentile	Q[m ³ /s]	V[m/s]	H _{upstream} [m]	H _{downstream} [m]	ΔHV[m]	Ph[kW]	Pt[kW]
95	3.1	1.7	235	140	95	7055	7055
50	3.7	2.1	218	140	78	7897	7897
5	4.3	2.4	200	140	60	8352	8352

Table 2: Recovered energy

Pt[kW]	Δt[h/year]	E [GWh/y]
7055	8760	62
7897	8760	69
8352	8760	73

In the table 1, the available mass flow rate values to be turbocharged are presented, as well as the respective available useful head and produced energy for an uninterrupted period of 365 days a year, for an ideal situation considering the efficiency of the turbomachine, η , equal to 100%.

By observing either figure 4 and table 1 we can note the relationship between flow speed and head losses in the valve, that is, as can be seen, for higher flow rates, higher speeds occur, and therefore higher losses, as postulated by Darcy-Weisbach in its roughness formula.

2 Technical Analysis: Evaluation of Recovered Energy

After processing the data of the occurrence of the different massflow rates, as well as verifying the existence of enough energy for the installation of a turbine in the circuit for the production of electric energy, in this section we have proceeded to the selection of the type of turbine to be installed.

The range of probability of occurrence of massflow rate of table 1 shows the massflow rate values at which the turbine must operate. These values are between 3.1 and 4.3 m³/s, and corresponds to the 95% and 5% percentiles, respectively; all massflow rates beyond these have a very low range probability of occurrence.

Thus, by crossing the corresponding data, obtained in the previous section, namely massflow rate and the minor head losses in the regulation valve, the type of turbine to be installed is determined by figure 5, in this case, a Francis turbine.

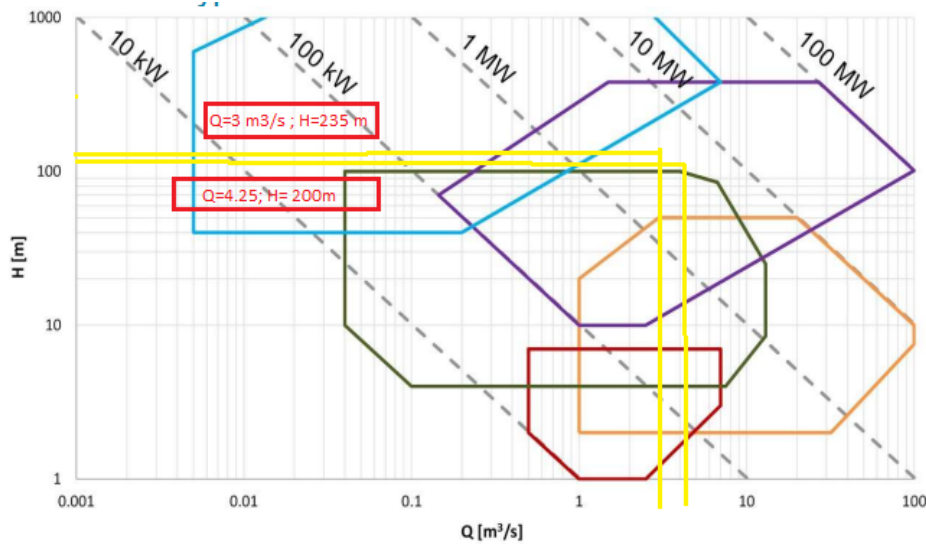


Figure 5: Turbine Selection Abacus.

Since a Francis turbine was selected, several calculations had to be carried out in order to find a function that better and more accurately expresses the actual behavior of the efficiency for the different massflow rates constant in the flow probability curve (Figure 2), as well as the respective turbined powers.

Figure 6 ($n_s=250$ rpm) presents the curve and the respective mathematical expression that describes the efficiency as a function of massflow rate ratio for the selected turbine.

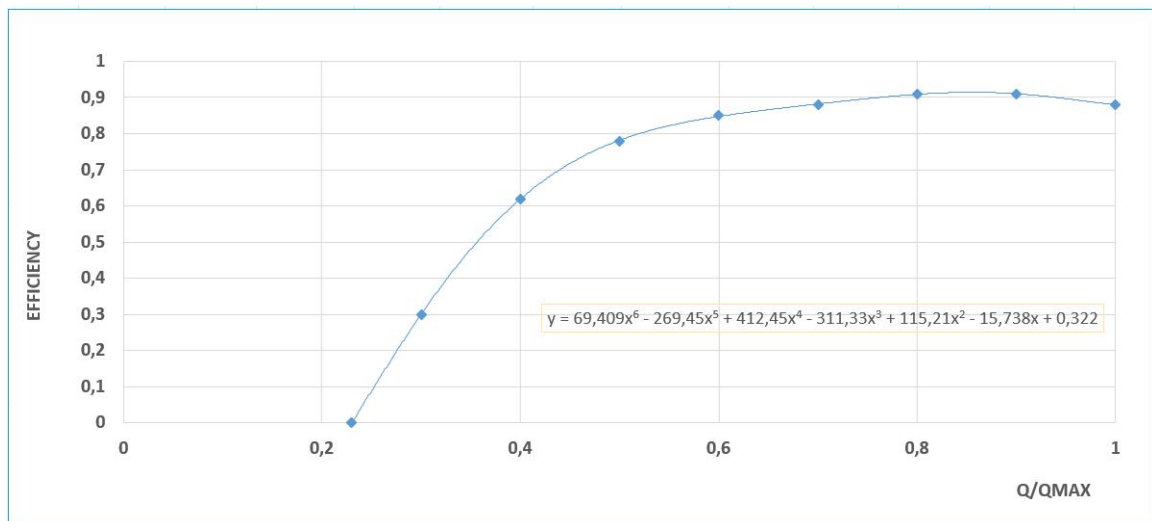


Figure 6: Approximation for turbine efficiency.

The selection of a Francis turbine leads us to establish limits for each of the design mass flow rates and height to be operated by the turbine. Thus, as can be seen, Table 2 shows the range of possible

design flow rates and useful drop, as well as the respective operating range for extreme situations, which correspond to intervals of 40% - 110% and 65%-125% for design flow and usable drop, respectively.

Table 3: Range of design mass flow rates and their heights.

Q_0	Q_{\min}	Q_{\max}	H_0	H_{\min}	H_{\max}
3	1.2	3.3	97.3	63.2	121.6
3.3	1.3	3.6	89.7	58.3	112.1
3.5	1.4	3.9	82.1	53.4	102.6
3.8	1.5	4.2	74.6	48.5	93.2
4	1.6	4.4	67	43.5	83.7
4.3	1.7	4.7	59.4	38.6	74.3
4.6	1.8	5	51.8	33.7	64.8
4.8	1.9	5.3	44.3	28.8	55.3

In opposition to the range of values shown in the mass flow probability of occurrence curve of figure 2, two values were added to it, whose tendency would be the same as the original points, in order to better assess the evolution of the produced energy as a function of the respective possible design mass flow values.

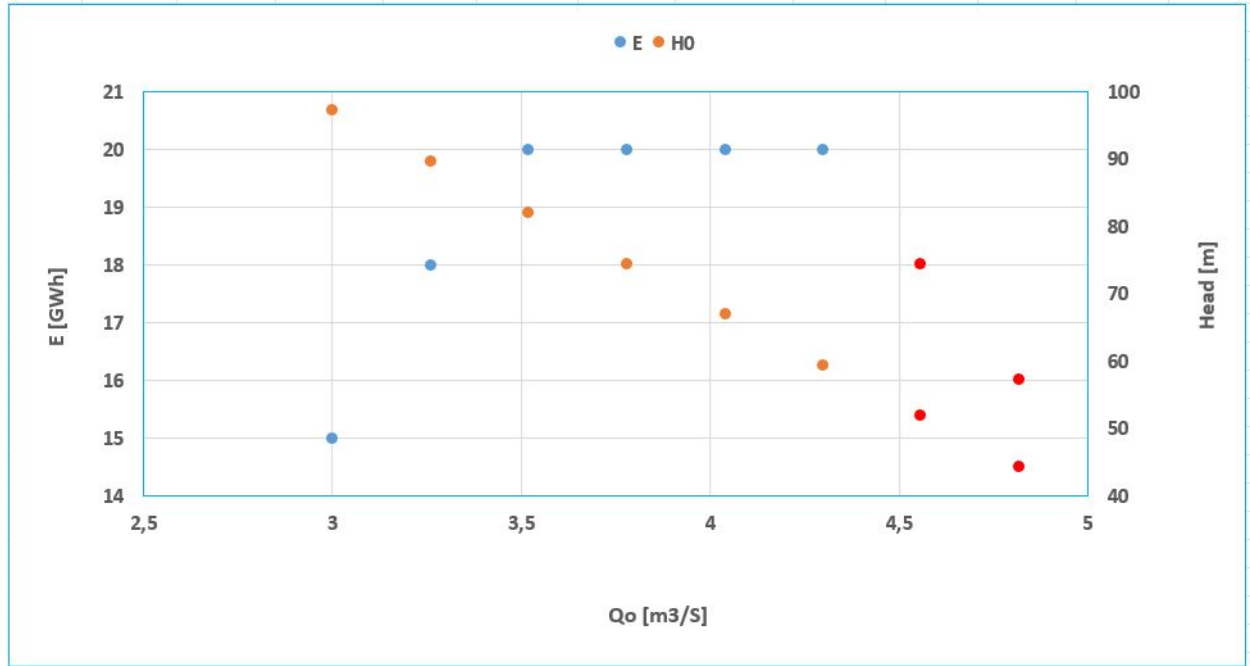


Figure 7: Energy produced according to design mass flow rates.

Based on the results in figure 7, the design flow leading to a maximization of recovered energy is $Q_0 = 3.52 \text{ m}^3/\text{s}$.

It is noteworthy that, for each iteration, whenever the mass flow rate is greater than the maximum design flow in question, this maximum is automatically assumed to operate the turbine. The same is true for the respective height values. On the other hand, for situations where the flow is lesser than the minimum design mass flow rate or the available height is lesser than the minimum operating height, the system will interrupt the operation of the equipment.

3 Economic Analysis

Once selected the right type of turbine in the previous section and knowing the respective efficiency, we were able to determine the power regarding to each design flow rate, as shown below:

Table 4: Range of design mass flow rates and their heights.

Q_0	H_0	E [GWh]	P_t [kW]
3	100	5	2651
3.3	94	6	2708
3.5	88	6.7	2724
3.8	81	6.7	2696
4	74	6.7	2621
4.3	66	6.7	2496
4.6	58	6	2318
4.8	49	5.3	2085

Then, by crossing the values of each design flow rate and using the different functions according to the available net we have obtained the capital cost in USD/kW, as shown in figure 8.

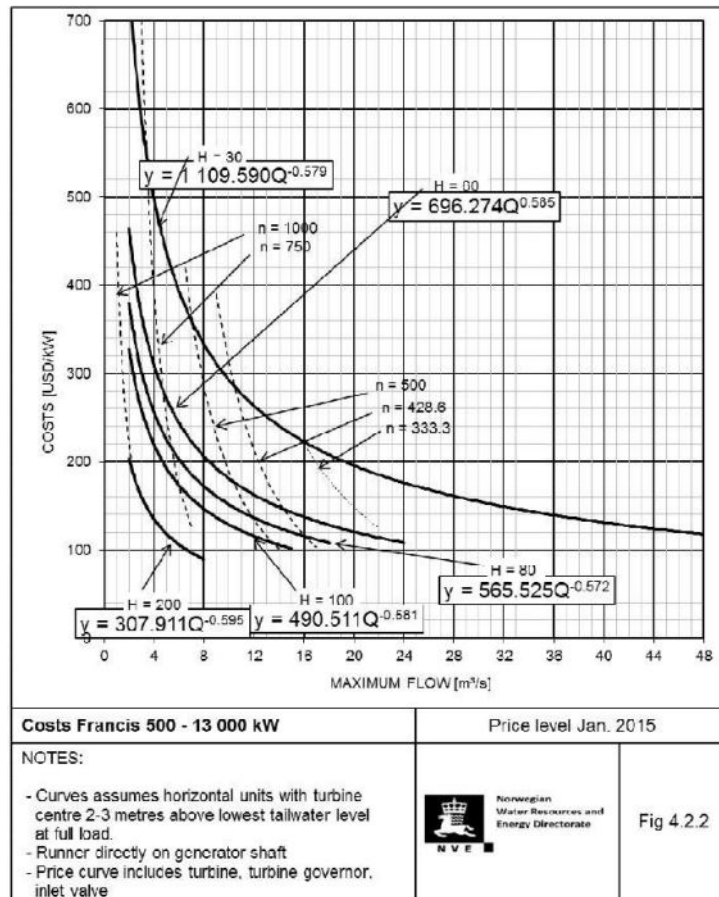


Figure 8: Capital cost abacus.

A conversion factor of 0.9 was applied to obtain the equivalent in our local currency (EUR). Additionally, both the civil works (installation) and the local accumulated discount rate were taken into account, with

1.9 and 1.6, respectively. The obtained values for the investments (capital costs) can be checked in the following table:

Table 5: Capital cost (investment).

Q_0	H_0	Inv[USD/kW]	Inv[EUR/kW]	Inv_CW[EUR/kW]	Inv_CW_ta[EUR/kW]	Inv[EUR]
3	100	259	233	443	709	1 878 919
3.3	94	247	222	422	675	1 828 857
3.5	88	236	212	404	646	1 759 399
3.8	81	264	238	452	723	1 949 315
4	74	254	229	435	696	1 824 333
4.3	66	297	267	507	812	2 025 426
4.6	58	287	258	490	784	1 817 910
4.8	49	277	250	474	759	1 583 042

Knowing the exact amount of the investment we have calculated the net benefits that includes the operation and maintenance costs (5% of investments) and the benefits of selling energy.
and so we could calculate the Payback period.

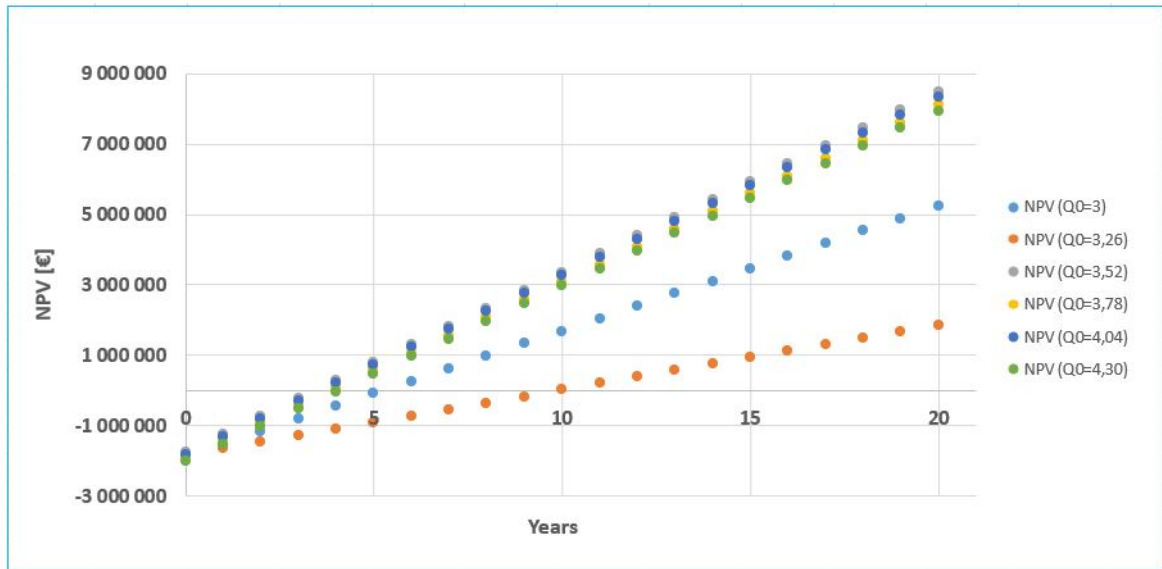


Figure 9: Payback period for each design flow rate.

By observing the figure ?? we can our optimal design discharge is the one that lead us to the maximum NPV, in our case it would be between 3.52 to 4.04. We can check the table ??, so we can be sure of the value:

Table 6: Range of design mass flow rates and their heights.

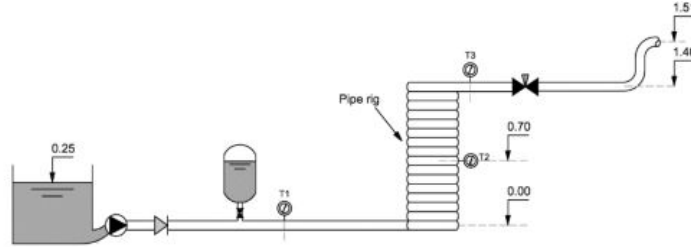
3	5
3.3	4.1
3.5	3.4
3.8	3.9
4	3.8
4.3	4.1

Now we can assert that our optimal design discharge is $3.5 \text{ m}^3/\text{s}$.

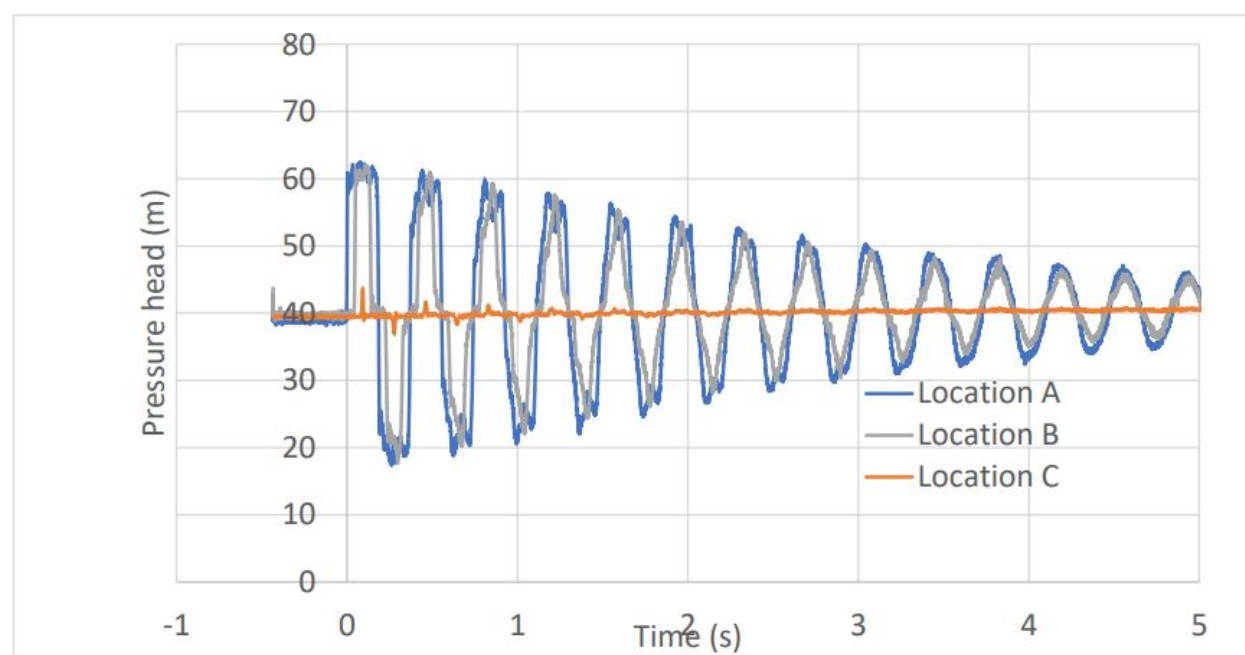
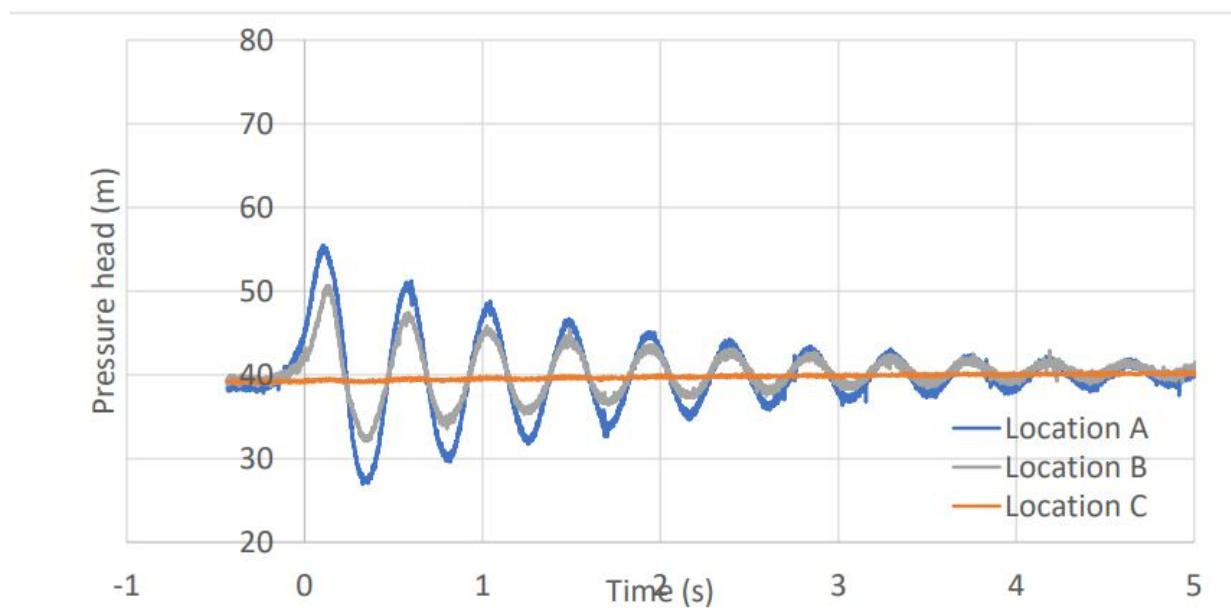
4 Hydraulic Transient Analysis

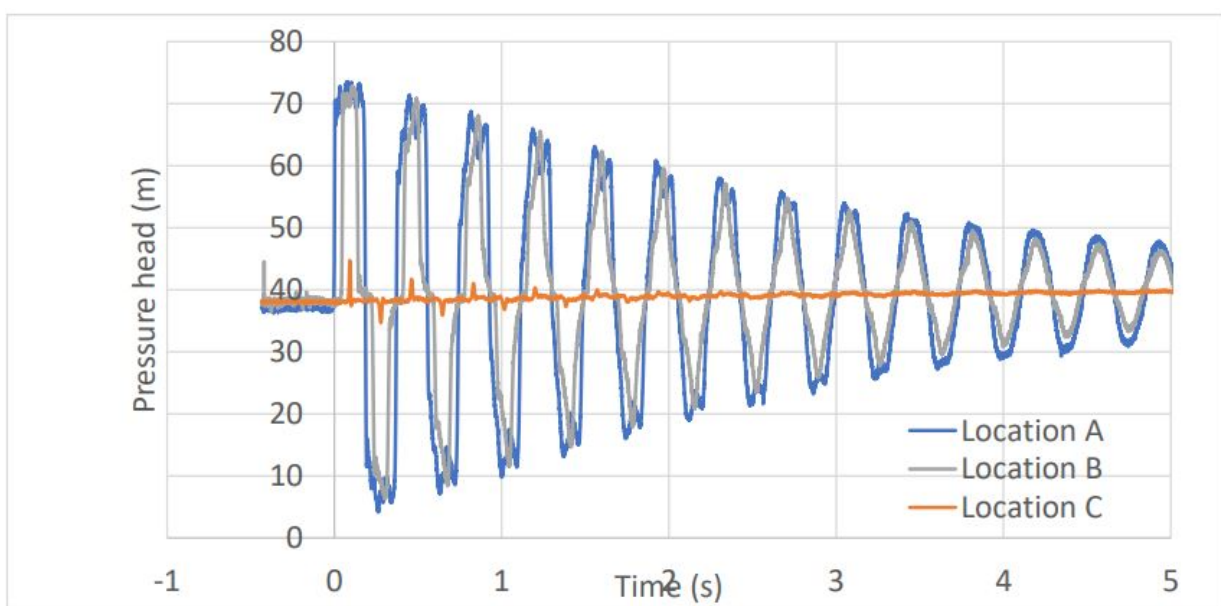
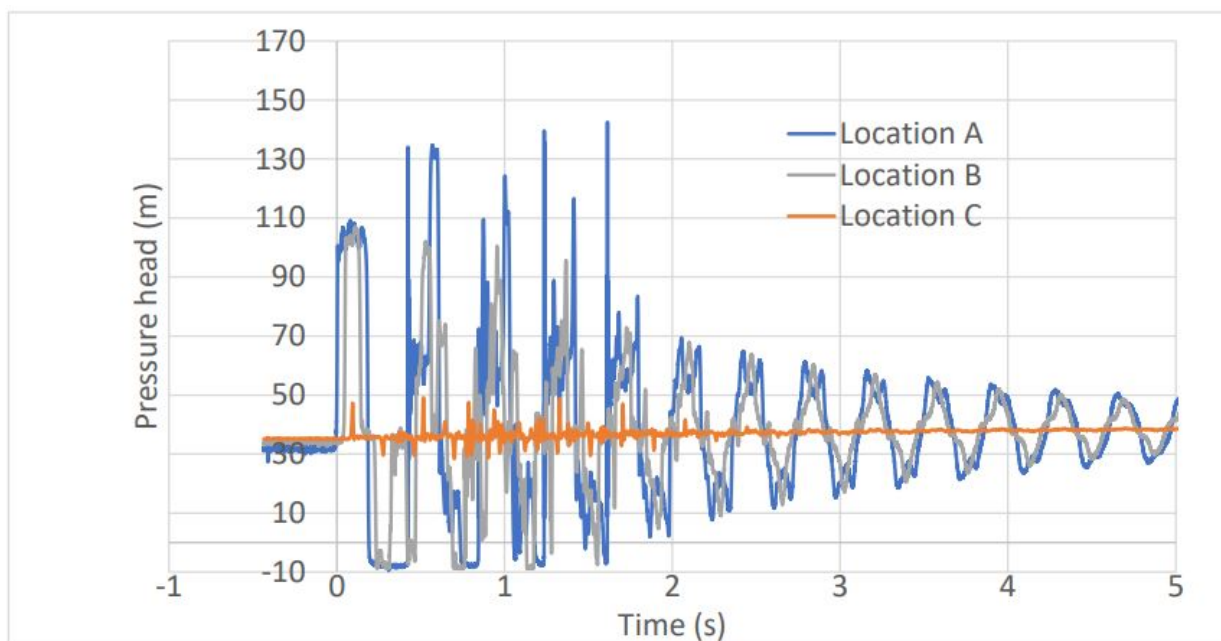
The system is fed from a 125-liter storage tank by a pump with a nominal flow rate of $1.0 \text{ m}^3/\text{h}$, a nominal head of 32.0 m , and a total power of 1.75 kW . A needle check valve is located immediately downstream of the pump and is used to prevent reverse flow through the pump. A hydro-pneumatic vessel with a capacity of 60 l is located downstream of the check valve. By opening or closing a ball valve, this device may be connected or detached from the main pipeline. At the downstream end of the pipe, there is a ball valve with DN $3/4"$ that allows the steady-state flow rate to be controlled. At 1.51 m from the facility's supporting frame's base, fluid is vented into the environment. An electromagnetic flowmeter measures steady-state flows, and three strain-gauge type pressure transducers (WIKA) with an absolute pressure range of 0 to 25 bar and an accuracy of 0.5 percent of full range measure transient-state pressures. The transient-state pressures are measured with a four-channel data collecting system (Picoscope). Transducers are placed in various portions of the pipe, including section T1 at the upstream end, section T2 in the center, and section T3 at the downstream end, with the fourth channel utilized to gather the initial flowrate.

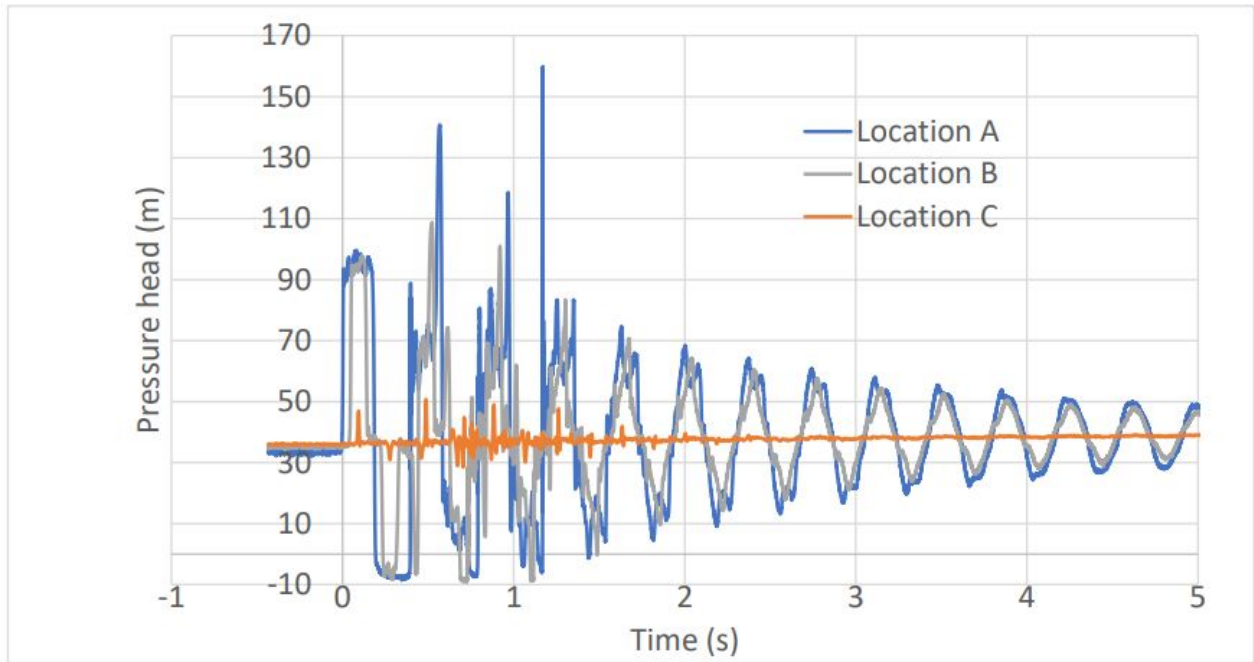
Coiled copper pipe length [m]	102.3
Inner diameter [mm]	20
Pipe-wall thickness [mm]	1
Storage tank [l]	125
Pump nominal flow rate [m^3/h]	1
Nominal head [m]	32
Total power [kW]	1.75
Hydro-pneumatic vessel [l]	60
Discharged pressure into atmosphere [m]	1.51



- Plot and analyse collected transient pressure data. We are going to consider and analyse the head pressure values referred to different initial flow rate simulations carried out using the valve manually. We will note the differences relative to the initial flow rate (set for Q208,Q330,Q596,Q693) and for all the ducts and different parts of the system, after which we will be able to give a logical definition of the operation of the system.





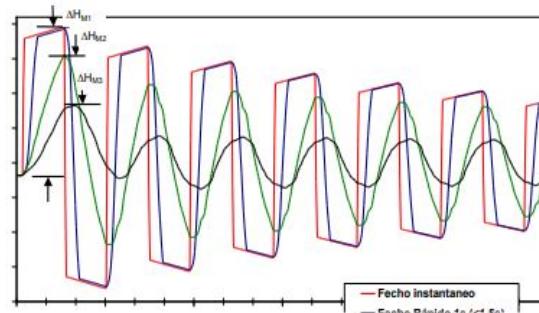


From these graphs, it can be seen that as the initial flow rate varies, the time-dependent response of the system is given by a peak and trough behaviour of the pressure head in the various locations of the system. The subdivision of the colours makes it possible to note how different parts of the system have different values in metres and how the trend is symmetrical with respect to the x-axis. The highest energy is located at the point where the impact between the fluid and the valve occurs, creating the highest pressure head and consequently energy. The value of d decreases as time passes, bringing the initial flow back into equilibrium. The speed of the pressure wave travelling through the pipes (called celerity) is one of the most crucial inputs to transient analysis. The speed is determined by the fluid characteristics and the pipe parameters, and it has a substantial influence on the size of the transient pressure wave and its speed through the pipes. The speed of a pressure wave in water, which is 4,716 ft/s (1,115 m/s), is commonly used to limit wave speed. However, there are various elements that might influence the speed. Helmholtz published the first equation for wave speed in 1848, which was later modified by Korteweg and is utilized in the HAMMER wave speed calculator.

$$a = \sqrt{\frac{E_v / \rho}{1 + \frac{D E_v \psi}{e E}}}$$

Where a = wave speed, m/s; E_v = bulk modulus of elasticity of liquid, Pa; E = Young's modulus for pipe material, Pa; ρ = fluid density, kg/m³; e = wall thickness, mm; D = pipe diameter, mm;

Pressure transients, surge, or water hammer are described as the occurrence of pressure and velocity changes in a closed conduit at the same time. Both long and short pipelines might experience water hammer. The greater and faster the shift in velocity, the greater the pressure changes.



Our next goal will be to create a transient study corresponding to the hydropower station's shutdown due to a failure in the electric grid, when running at the design discharge and with no surge protection. The goal is to imitate a turbine halt by closing the valve many times (0, 10, 60 and 120 s). As a result, we must estimate the minimum wicket closure duration such that it does not exceed 20% of the maximum static pressures or produce pressures below atmospheric pressure in the same system. And we'll see that for each circumstance, calculating the temporal variation of the piezometric head and discharge at the pipe segment directly upstream of the hydropower plant will be useful. Hydraulic transients, also known as pressure surges, are caused by abrupt changes in flow rates in pumping and pipeline systems. The pressures generated may be strong enough to cause pipeline damage or perhaps catastrophic breakdown. Specialized hydraulic transient analysis serves as the foundation for developing surge control methods to protect critical infrastructure. All these analysis procedures are carried out through the use of a commercial software Hammer, which has the task of simulating our system and calculating, by means of known input values, the total response in order to estimate the correct functioning of the system. We will then see graphical trends describing different simulations set up and the behaviour of the various valve closures in different time intervals, which will allow us to study different trends and different responses from the system.

The next tables represent the variables and characteristics that described the lab analysis:

k	2.19E+09
rho	1000
alfa	0.91
Poisson	0.3
D [m]	1.5
e [m]	0.017
E0 [Pa]	2.07E+11
D/e	88.23529

a [m/s]	1088.169
Deltat [s]	0.01

	L	D	a	X	Number	Adj.Length
Pipe1	35616	1.5	1100	11	3237.818	35618
Pipe2	7	1.5	1100	11	0.636364	11
Pipe3	8	1.5	1100	11	0.727273	11
Pipe4	9	1.5	1100	11	0.818182	11

0sec	64.76	[s]	Fast	delta_Hj	270.31	[m]
10sec	64.76	[s]	Fast	delta_Hj	270.31	[m]
60sec	64.76	[s]	Slow	delta_Hm	1050314	[m]
120sec	64.76	[s]	Slow	delta_Hm	210062.7	[m]

Q_i	4.26	[m3/s]		Pipe	Length
A	1.767146	[m2]		P1	35618
V0	2.410667	[m/s]		P2	11
g	9.81	[m/s^2]		P3	11
				P4	11

